IOP Conference Series: Materials Science and Engineering

PAPER • OPEN ACCESS

Inquiry of inclined magnetic field effects on Walter –B nanofluid flow with heat generation / absorption

To cite this article: K Loganathan *et al* 2020 *IOP Conf. Ser.: Mater. Sci. Eng.* **872** 012097

Inquiry of inclined magnetic field effects on Walter –B nanofluid flow with heat generation / absorption

K Loganathan[1*], N Nithyadevi[1], P Boopathi[2] and K Mohana[3]

[1]Department of Mathematics, Faculty of Engineering, Karpagam Academy of Higher Education, Coimbatore - 641021, Tamil Nadu, India.

[2]Department of Mathematics, Rathnavel Subramaniam College of Arts & Science, Coimbatore-641402, Tamil Nadu, India

[3]Department of Mathematics, Sasuri College of Engineering, Tirupur 638056, Tamil Nadu, India .

[*]*Email:loganathankaruppusamy304@gmail.com*

Abstract: The article deals with Walter-B nanoliquid flow towards a extending surface with inclined magnetic field effects. Thermal relaxation analysis is made by non fourier heat flux model. Radiation, heat generation / absorption impacts are included. The non linear Partial governing systems are rebuild into nonlinear ordinary systems with the assist of proper similarity transformations. The graphical results are portrayed for velocity, concentration and temperature profile. The physical entitles of heat and mass transfer rates are graphically reported. The comparission with previous results notified the excellent agreement.

Key words: Walter-B nanofluid, Inclined magnetic field, Radiation, Brownian motion.

1. Introduction

Magnetohydrodynamic (MHD) flow has a limitless number of practical and theoretical researches in numerous geophysical, physical and industrial segments. Mostly the MHD flows associated with heat transmission have acquired substantial consideration up to now. It is due to the interest that usages of MHD flows occur in many manufacturing areas like nuclear reactor cooling, microelectronic tools, electronic packages, etc. To author's knowledge, MHD flow caused by a stretched wall is examined by Pavlov [1]. He obtained the exact analytic solution in the apperance of a uniform magnetic field. Moreover, some imperative impacts in MHD flow with heat transmission were done by ref's [2]-[10]. Mostly the cooling liquids have the constant physical properties that are considered from the previous data. In practical situations the variable characteristics with physical propertiesare important. Hayat et al. [11] explored the 3D flow of Jeffry fluid flow in the appearance of variable thermal conductivity. Bhattacharyya et al. [12] consider the temperature-dependent viscosity with the boundary layer slip flow due to stretchy sheet. The impact of the combined convective flow of viscous fluid embedded in a porous surface is explored by Hayat et al. [13]. Rashidi et al. [14] studied the MHD flow of a fluid over a rotating disk. They use a numerical way to obtain the results also examine the influence of magnetic interaction number. Pal and Mondal [15] presented the MHD forced convection through a wedge with thermal radiation temperature-dependent viscosity. Pal and Mondal [16] additionally described variable thermal conductivity and temperature-dependent viscosity effects in MHD stretchy non-Darcy combined the convective flow of species.

This study addressed the 2D flow of Walter-B nanofluid flow across a convective surface with radiation and heat generation effects. Nanomaterial includes Brownian motion and thermophoresis

impacts. The homotopy analysis technique (HAM) [16-21] is applied to solve the nonlinear function of ODE. Results of velocity, nanoparticle concentration, and temperature are produced via graphical representation. Code validation with formerly published results is obtained good agreement.

2. Mathematical formulation of the problem

We examine the flow of 2-D incompressible laminar boundary layer flow of Walter-B nano liquid flow towards a shrinking plate. The non Fourier heat flux is taken into account. Radiation, heat genration and convective heating effects are included. The two tempertures $\mathbf{T_W}$ and $\mathbf{T_\infty}$ are on and apart from thesurface. The applied magnetic field $\boldsymbol{B_m}$ is implimented in positive y- direction. The governing equations are defined with the help of Figure. 1.

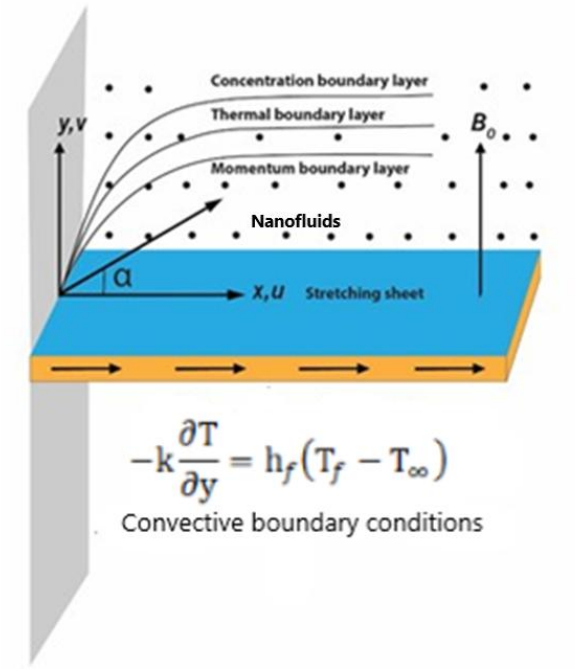

Figure.1 Flow geometry

$$\frac{\partial u}{\partial x}+\frac{\partial v}{\partial y} = 0 \quad (1)$$

$$u\frac{\partial u}{\partial x} + v\frac{\partial u}{\partial y} = \nu\frac{\partial^2 u}{\partial y^2} - \frac{k_0}{\rho}\left[u\frac{\partial^3 u}{\partial y^2 \partial x} + v\frac{\partial^3 u}{\partial y^3} + \frac{\partial u}{\partial x}\frac{\partial^2 u}{\partial y^2} - \frac{\partial u}{\partial y}\frac{\partial^2 u}{\partial x \partial y}\right] - \frac{\sigma B_m^2}{\rho} sin^2\alpha\, u \quad (2)$$

$$u\frac{\partial T}{\partial x} + v\frac{\partial T}{\partial y} = \frac{k}{\rho c_p}\frac{\partial^2 T}{\partial y^2} - \frac{1}{\rho c_p}\frac{\partial q_r}{\partial y} + \frac{Q_0}{\rho c_p}(T - T_\infty) + \tau\left[D_B\frac{\partial C}{\partial y}\frac{\partial T}{\partial y} + \frac{D_T}{T_\infty}\left(\frac{\partial T}{\partial y}\right)^2\right] \quad (3)$$

$$u\frac{\partial c}{\partial x} + v\frac{\partial c}{\partial y} = D_B\frac{\partial^2 c}{\partial y^2} + \frac{D_T}{T_\infty}\frac{\partial^2 T}{\partial y^2} \quad (4)$$

$$u = U_w(x) = ax, v = v_w, -k\frac{\partial T}{\partial y} = h_f(T_f - T_\infty), \qquad C = C_w \; at \; y = 0$$

$$u \to 0, v \to 0, T \to T_\infty, C \to C_\infty as\; y \to \infty (5)$$

Applying Cattaneo-Christov theory we get:

$$u\frac{\partial T}{\partial x}+v\frac{\partial T}{\partial y}+\lambda_T\left(u^2\frac{\partial^2 T}{\partial x^2}+v^2\frac{\partial^2 T}{\partial y^2}+\left(u\frac{\partial u}{\partial x}+v\frac{\partial u}{\partial y}\right)\frac{\partial T}{\partial x}+2uv\frac{\partial T^2}{\partial x\partial y}\right)$$
$$+\left(u\frac{\partial v}{\partial x}+v\frac{\partial v}{\partial y}\right)\frac{\partial T}{\partial y}=\frac{k}{\rho c_p}\frac{\partial^2 T}{\partial y^2}-\frac{1}{\rho c_p}\frac{\partial q_r}{\partial y}+\frac{Q_0}{\rho c_p}(T-T_\infty)+\tau\left[D_B\frac{\partial C}{\partial y}\frac{\partial T}{\partial y}+\frac{D_T}{T_\infty}\left(\frac{\partial T}{\partial y}\right)^2\right] \quad (6)$$

The similarity transformation are:

$$\psi=\sqrt{a\nu}xF(\zeta), u=\frac{\partial\psi}{\partial y}, v=-\frac{\partial\psi}{\partial x}, \zeta=\sqrt{\frac{a}{\nu}}y, u=axF'(\zeta), v=-\sqrt{a\nu}F(\zeta),$$

$$\theta(\zeta)=\frac{T-T_\infty}{T_f-T_\infty}, \phi(\zeta)=\frac{C-C_\infty}{C_w-C_\infty}. \quad (7)$$

Eqns (2), (4), (6) and (7) taken into the form

$$F'''-F'^2+FF''+We\left(2F'F'''-FF^{iv}-F''^2\right)-Ha^2sin^2\alpha\,F'=0 \quad (8)$$

$$\left(1+\frac{4}{3}R\right)\theta''+PrF\theta'+PrQ\theta-Pr\delta(F^2\theta''+FF'\theta')+PrNb\,\theta'\phi'+PrNt\theta'^2=0 \quad (9)$$

$$\phi''+LeF\phi'+\frac{Nt}{Nb}\theta''=0 \quad (10)$$

with boundary conditions

$$F(\zeta)=F_w, F'(\zeta)=1,\ \theta'(\zeta)=-\lambda(1-\theta(0)),\ \phi(\zeta)=1 \text{ at } y=0 \quad (11)$$

The dimensionaless variablesare stated as:

$$We=\frac{k_0a}{\rho}, Ha^2=\sqrt{\frac{\sigma B_m^2}{\rho a}}, \Pr=\frac{\rho c_p}{k}, R=\frac{4\sigma^*T_\infty^3}{kk^*}, Q=\frac{Q_0}{\rho c_p}, \lambda=\frac{h_f}{k}\sqrt{\frac{\nu}{a}},$$

$$\delta=\lambda_T a, Nb=\frac{\tau D_B}{\nu}(C_w-C_\infty), Nt=\frac{\tau D_T}{\nu}\left(T_f-T_\infty\right)$$

The dimensionless forms ofphysical entitles are

$$Re^{\frac{1}{2}}CF_x=(1-We)F''(0)-F_wF'''(0)$$
$$Re^{-\frac{1}{2}}Nu_x=-\left(1+\frac{4}{3}R\right)\theta'(0),$$
$$Re^{-\frac{1}{2}}Sh_x=-\phi'(0)$$

3. Solution technique (HAM)

The initial assumptions for homotopy procedure are stated as
$\boldsymbol{F_0 = F_w + 1 - e^{-\eta}}$,

$$\boldsymbol{\theta_0 = \frac{\lambda * e^{-\eta}}{1 + \lambda}}$$

$\boldsymbol{\phi_0 = e^{-\eta}}$.
The auxiliary linear operators $\boldsymbol{\mathcal{L}_F}$, $\boldsymbol{\mathcal{L}_\theta}$ and $\boldsymbol{\mathcal{L}_\phi}$ are derived as
$\boldsymbol{\mathcal{L}_F = F'(\eta)(F''(\eta) - 1)}$,

$$\boldsymbol{\mathcal{L}_\theta = \theta''(\eta) - \theta(\eta)}$$
$$\boldsymbol{\mathcal{L}_\phi = \phi''(\eta) - \phi(\eta)}$$

with satisfying the following properties
$\boldsymbol{\mathcal{L}_F[\Omega_1 + \Omega_2 e^{\eta} + \Omega_3 e^{-\eta}] = 0}$,

$$\boldsymbol{\mathcal{L}_\theta[\Omega_4 e^{\eta} + \Omega_5 e^{-\eta}] = 0}$$
$$\boldsymbol{\mathcal{L}_\phi[\Omega_6 e^{\eta} + \Omega_7 e^{-\eta}]}$$

where $\boldsymbol{\Omega_j (j = 1 - 7)}$ denote the arbitrary conditions.
The appropriate solutions $[\boldsymbol{F_m^*, \theta_m^*, \phi_m^*}]$ are

$$F_m(\eta) = F_m^*(\eta) + \Omega_1 + \Omega_2 e^{\eta} + \Omega_3 e^{-\eta}$$
$$\theta_m(\eta) = \theta_m^*(\eta) + \Omega_4 e^{\eta} + \Omega_5 e^{-\eta}$$
$$\phi_m(\eta) = \phi_m^*(\eta) + \Omega_6 e^{\eta} + \Omega_7 e^{-\eta}$$

4. Results and discussion

In this section we examined the impacts of different flow parameters over velocity, nanoparticle concentration, and temperature. The homotopy technique (HAM) is implimented for solve the nonlinear systems and the results are presented through graphically.
Figures.2&3 displays the impression of α and F_w on the velocity distribution. It is observed that the velocity distribution and its related boundary layer thickness diminishes by increasing α and F_w. Figure.4 represents the differences in the velocity field with an increase in Weissenberg number We. It is examined that the velocity falls with a rise in Weissenberg number We. Conversely, the momentum boundary layer also weakens when Weissenberg number We is enhances. Substantially, rising values of Weissenberg number We upsurges tensile stresses which oppose the momentum transport and therefore boundary layer thickness reduces.The influence of Hartmann number Ha on the velocity profile F' are portrayed in Figure. 5. The applied magnetic field has the movement to reduce speed of the liquid which diminishes the velocity profile.

Figure. 6 sketched for various values of Hartmann number Ha. By way of Lorentz force is a resistive force which go up against the liquid motion thus heat is formed and subsequently thermal boundary layer thickness growths.Here $\delta = 0$specifies the consistent outcomes for the classical Fourier's law. Impact of thermal relaxation time for heat flux δ on the temperature profile is investigated in Figure. 7. It is noted that Catteno-Christov heat flux is smaller then the normal heat flux. Figures. 8 & 9 describes that wide range of radiation (R) and Heat generation (Q)constants on temperature profile the thermal and momentum boundary layer thickness rises for large values of R & Q. Figures. 10 & 11 demonstrates the effect of the Biot number (λ) and suction/injection parameter (F_w) on temperature profile. Thus, we decided that the thermal boundary layer thickness has the improvement in rising the Biot number and it reduces with enhancing the suction/injection parameter.

Effects of Brownian ($Nb = 0.0, 0.5, 1.0, 1.5, 2.0$) and thermophoresis ($Nt = 0.1, 0.6, 1.2, 1.8, 2.5$) on temperature are shown in Figures. 12 & 13. Here temperature is an growing function of both variables. For an improvement in these variables the temperature upsurges. Brownian motion variable generates micro-mixing which augments the thermal performance of base liquid. Additionally, at nanoscale and molecular stages the Brownian motion of nanoparticles is a mechanism of nanoscale leading their thermal performance. In classification of nanofluid, Brownian motion occurs by the size of

nanoparticles which can affect the properties of heat transmission. Brownian motion of the particles and its impression on nearby liquids plays substantial role in heat transmission when size of particles tends to nanometerscale.

The effect of Nt and Nb on $\phi(\zeta)$ is exposed in Figures. 14 & 15, respectively. As it is displayed in these figures, nanofluid parameters have reverse impacts on the concentration profiles, that is, with enhancing thermophoresis parameter the nanoparticle concentration and their associated boundary thickness rises but higher rates of Brownian motion parameter tend to lesser the $\phi(\zeta)$ values. Physically, rising the thermophoresis parameter results in augmentation of thermophoresis energy that indicates nanoparticles moving from hot to cold parts and as a result, size of nanoparticle volume fraction increases. Furthermore, increasing Brownian motion parameter results in diminishing the diffusion of nanoparticles into the liquid regime apart from the surface, then $\phi(\zeta)$ decreases in the boundary layer.

From Figures. 16 & 17 shows the influence of local heat and mass transfer rates individually. Figure. 16 shows the heat transfer rate with the combination We and δ. Heat transfer rate reduces for higher values of Weissenberg number and thermal relaxation time constant. Figure. 17 depicts that the effect of mass transfer rate with the combination of Nb, Nt and Ha. It conclude tha Brownian motion and thermophoratic parameters showes the inverse efffect on mass transfer rate. Table. 1 displays the code validation of skin friction for previously reported results in ref [16].

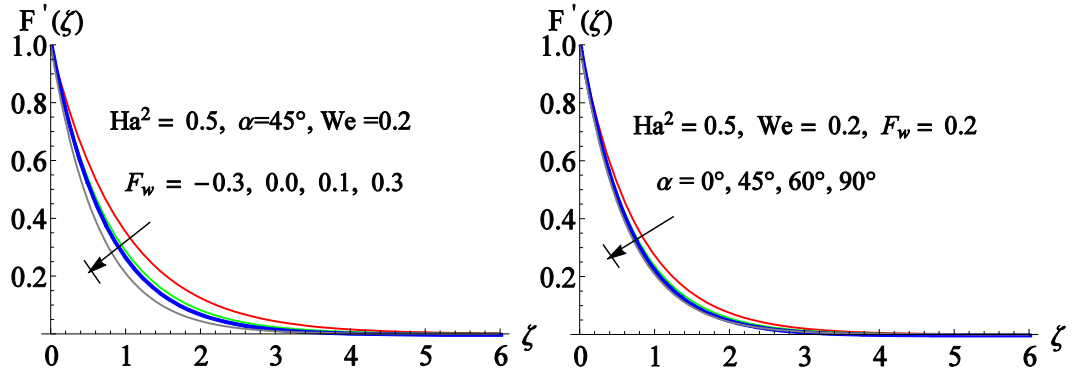

Figures.2 & 3 Impact of F_w and α on velocity field

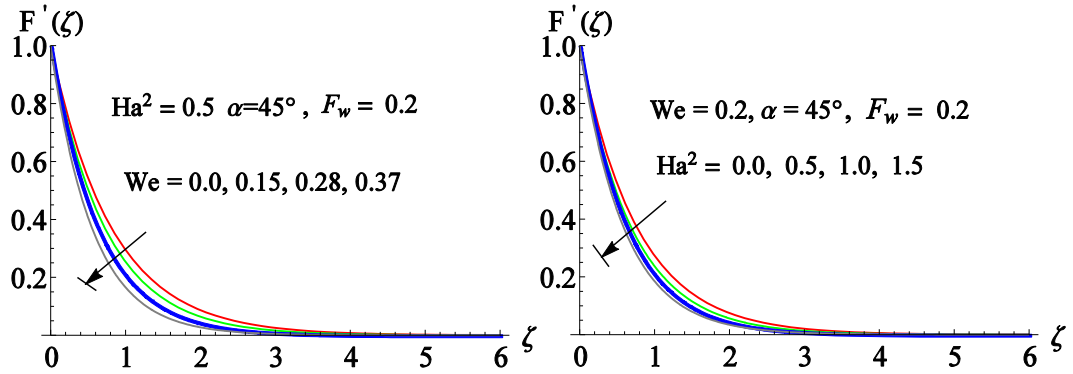

Figures. 4 & 5 Impact of We and **Ha** on velocity field

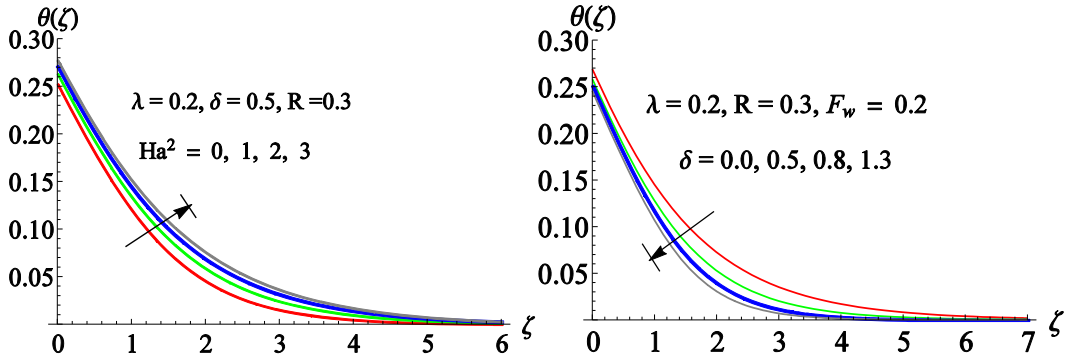

Figures. 6 & 7 Impact of **Ha** and $\boldsymbol{\delta}$ on temperature field

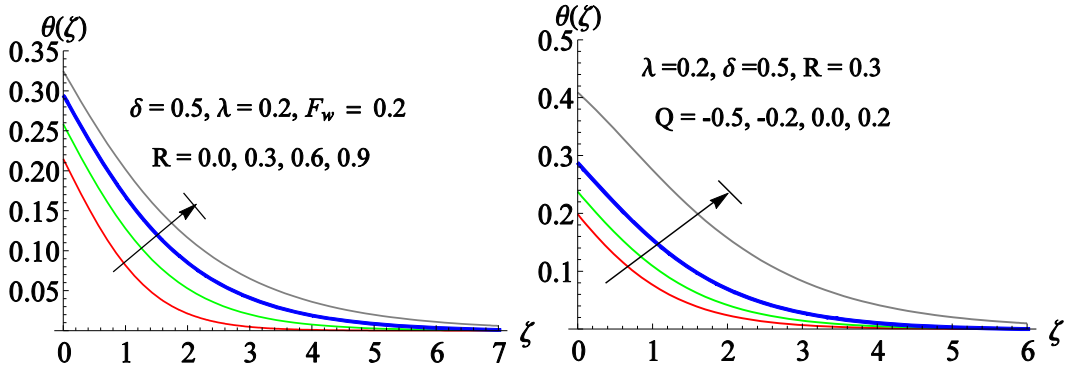

Figures. 8 & 9 Impact of R and Q on temperature field

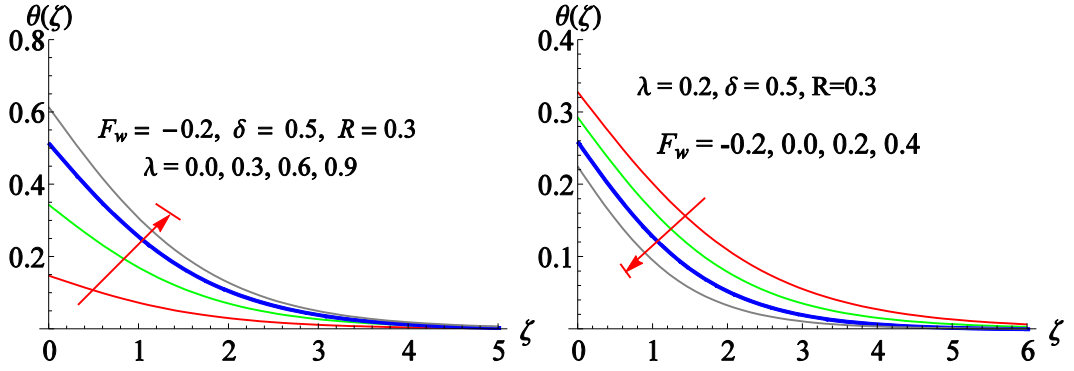

Figures. 10 & 11 Impact of F_w and λ on temperature field

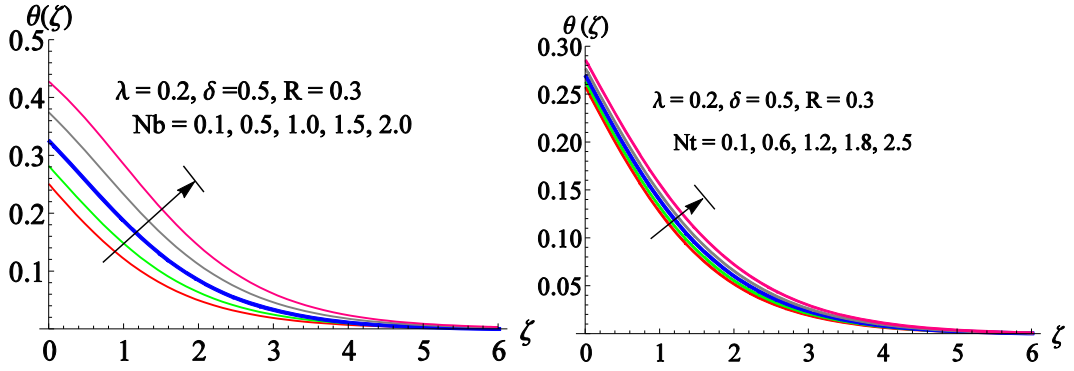

Figures. 12 & 13 Impact of Nb and Nt on temperature field

Table. 1 The comparission of $Re^{\frac{1}{2}}CF_x$ for different values of F_w and We when $Ha = 0$

F_w	We	Hayat[16]	Present
0.0		0.870726	0.870726
0.2		0.849053	0.849053
0.4		0.712725	0.712725
0.6		0.364968	0.364968
	0.0	1.2198	1.2198
	0.1	1.01937	1.01937
	0.2	0.712725	0.712725

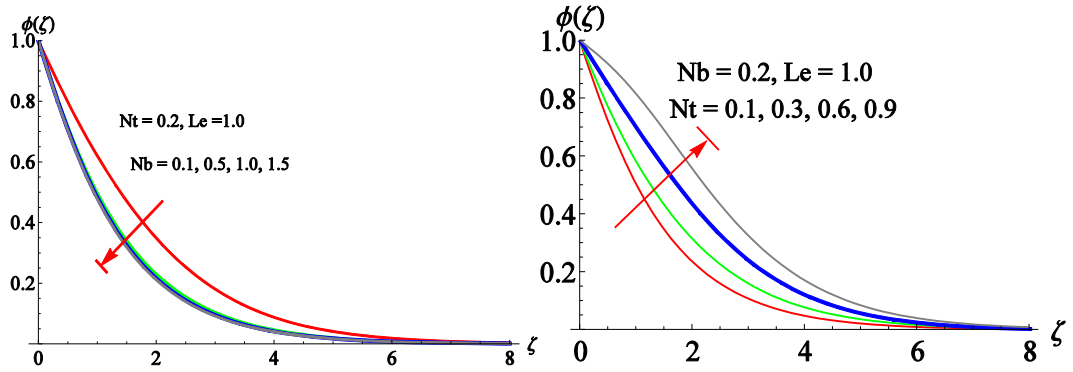

Figures. 14 & 15 Impact of Nb and Nt on concentration field

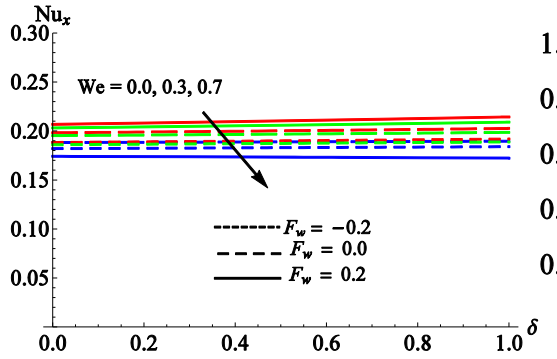

Figure. 16 Impact of We and δ onNu_x

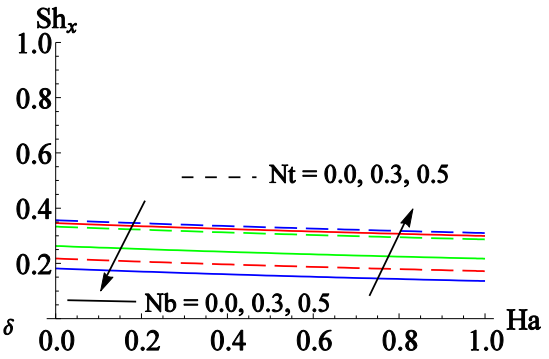

Figure. 17 Impact of Nb, Nt and Ha on Sh_x

5. Main outcomes

From the present examination the main observations are noted below:

- Velocity profile has reducing performance for higher We.
- Temperature profile reduces for higher thermal relaxation time constant.
- Larger values of Nt and Nb rises the temperature profile
- Nt and Nb shows the opposite effect on the concentration and Sherwood number profiles. .
- Heat transfer rate reduces via Weissenberg number We.

References

[1]. Pavlov KB (1974) Magnitnaya Gidrodinamiks, Sudan.
[2]. Hayat T, Shafiq A, Alsaedi A, and Awais M. (2013) *Comput Fluids*, **86(5)**103-108.
[3]. Ramzan R, Farooq M, Alsaedi A, and Hayat T. (2013) *Eur. Phys. J. Plus*, **128(5)** 1-15.

[4]. HayatT, Shafiq A, AlsaediA, and AsgharS. (2015) *AIP Adv*,**5(8)** 087108.
[5]. Bhattacharyya K, Mukhopadhyay S, and Layek GC. (2012)*Chem Eng Commun*,**199(3)** 368-383.
[6]. Turkyilmazoglu M. (2013) *Int J Mech Sci*, **77** 263-268.
[7]. Turkyilmazoglu M. (2014) *Int. J. Heat Mass Transfer*, **78** 150-155.
[8]. Pal D, and MondalH. (2013) *J Magn mater*, **331** 250-255.
[9]. Pal D, and Mondal H. (2011) *Commun. Nonlinear. Sci. Numer. Simul*, **16(4)**1942-1958.
[10]. Hayat T, Shafiq A, and Alsaedi A. (2014*) PLoS ONE*, **9(1)**e83153.
[11]. Hayat T, Shehzad SA, and Alsaedi A. (2013) *Appl Math Mech*, **34(7)** 823-832.
[12]. Bhattacharyya K, Layek GC, and Gorla RSR. (2013) *Thermal Energy and Power Engineering*, **2(1)** 38-43.
[13]. Hayat T, Shehzad SA, Qasim M, and Alsaedi A. (2014)*Braz. J. Chem. Eng*, **31**109-117.
[14]. Rashidi MM, Kavyani N, and Abelman S, (2014) *Int. J. Heat Mass Transfer*, **70**892–917.
[15]. Pal D, and Mondal H. (2009) *Appl Math Comput*, **212(1)** 194-208.
[16]. Hayat T, Asad S, Mustafa M, and Hamed Alsulami H (2014*) Chin. Phys.* B **23(8)** 084701
[17]. LiaoS, TanYA, (2007) *Stud Appl Math.* **119** 297–354
[18]. Loganathan K, Rajan S,(2020) *J Therm Anal Calorim*, DOI: 10.1007/s10973-020-09414-3
[19]. Loganathan K, Mohana K, Mohanraj M, Sakthivel P, and Rajan S(2020) *J Therm Anal Calo rim.*DOI: 10.1007/s10973-020-09751-3.
[20]. Loganathan K, Prabu K M, Elanchezhian E, Nirmalkumar R and Manimekalai K,(2020) *J. Phys: Conf. Ser.* **1432**012048.
[21]. LoganathanK, Sivasankaran S, Bhuvaneshwari M, Rajan S, (2019) *J Therm Anal Calorim.***136** 401- 409.